Evaluation of the impact of a scanner prototype on proton CT and helium CT image quality and dose efficiency with Monte Carlo simulation

S Götz[1], J Dickmann[1], S Rit[2], N Krah[2,3], F Khellaf[2], R Schulte[4], K Parodi[1], G Dedes[1,*], and G Landry[5,6,1,*]

[1]Ludwig-Maximilians-Universität München,[2] University of Lyon, [3]IP21 Lyon, [4]Loma Linda University, [5]University Hospital LMU Munich, [6]German Cancer Consortium (DKTK)

*equal contribution

3rd Ion Imaging Workshop

13th-14th October 2022

Image acquisition for modern particle therapy treatment planning

X-ray CT

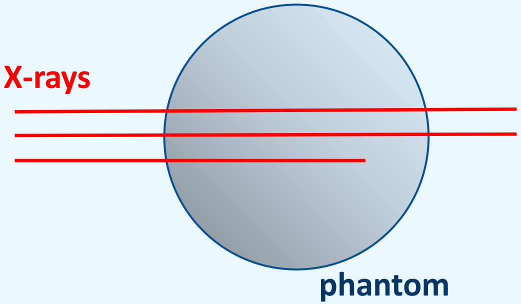

$$\int_{\text{path}} \mathrm{d}x\, \mu = \ln \frac{I}{I_0} \xrightarrow[\text{3.5\% uncertainty}]{\text{look up table}} \text{RSP}$$

- High uncertainties in the conversion of the photon attenuation coefficient μ to the corresponding RSP values using look-up tables and stochiometric calibrations

Ion CT

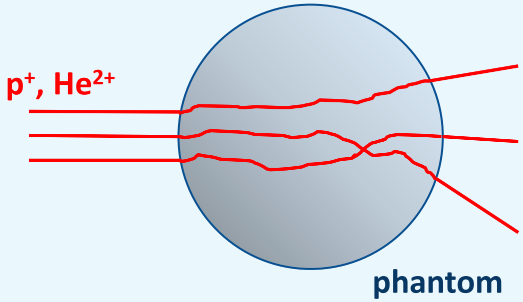

$$\int_{\text{path}} \mathrm{d}x\, \text{RSP} = \int_{E_2}^{E_1} \frac{\mathrm{d}E}{S^w} = \text{WEPL}$$

- Uncertainties below 1% achievable due to a more direct reconstruction of the RSP and accounting for curved paths in the reconstruction algorithm (MLP formalism and distance driven binning)

Imaging requirements

- Low image variance and imaging noise
- High spatial resolution
- Low imaging dose
- High RSP accuracy

How do protons and helium ions compare ?

What do we expect from theory?

Range

Bethe-Bloch stopping power $\frac{dE}{dx} = \frac{z^2}{f_S\left(\frac{E}{M}\right)}$

Range $R = \int_E^0 \left(\frac{dE}{dx}\right)^{-1} dE = \frac{M}{z^2} f_R\left(\frac{E}{M}\right) \Rightarrow \boxed{\frac{R_{He}}{R_p} = \frac{M_{He}}{M_p}\frac{z_p^2}{z_{He}^2} = 1}$

Variance / dose

Energy and **range straggling** $\sigma_E^2 = z^2 f_E\left(\frac{E}{M}\right)\Delta x$ & $\sigma_R^2 = \int_0^E \left(\frac{d\sigma_E^2}{dx}\right)\left(\frac{dE}{dx}\right)^{-3} dE$

$$\frac{\sigma_R}{R} = \frac{1}{\sqrt{M}} f_{R2}\left(\frac{E}{M}\right) \Rightarrow \boxed{\frac{\sigma_{R,He}^2}{\sigma_{R,p}^2} = \frac{M_p}{M_{He}} = \frac{1}{4}}$$

Dose deposition $D \sim \frac{dE}{dx} = \frac{z^2}{f_S\left(\frac{E}{M}\right)} \Rightarrow \boxed{\frac{D_{He}}{D_p} = \frac{z_{He}^2}{z_p^2} = 4}$

Nuclear reactions result in a loss of about 14% of protons and 29% of helium ions when traversing 150mm water

Image variance ratio for same dose $\boxed{\frac{V_{He}}{V_p} = \frac{N_p}{N_{He}}\frac{\sigma_{R,He}^2}{\sigma_{R,p}^2} = \frac{4}{1}\frac{0.86}{0.71}\frac{1}{4} = 1.2}$

Spatial resolution

Highland formula for scattering

$$\sigma_\theta = \frac{E_0}{\beta pc} z \sqrt{\frac{x}{X_0}}\left[1 + 0.038 \ln\left(\frac{x}{X_0}\right)\right] \sim \frac{z}{M} f_H\left(\frac{E}{M}\right) \Rightarrow \boxed{\frac{\sigma_{\theta,He}}{\sigma_{\theta,p}} = \frac{M_p}{M_{He}}\frac{z_{He}}{z_p} = \frac{1}{2}}$$

	pCT	HeCT
Energy E	200 MeV	800 MeV
Mass M	1 u	4 u
Specific energy E/M	200 MeV/u	200 MeV/u
Charge number z	1	2

- Due to the same specific energy, protons and helium ions will have the same **particle range**
- The **image variance** originates from energy/range straggling. For the same **imaging dose**, the helium image variance is expected to be about 20% higher than the proton image variance due to the loss of particles in nuclear interactions
- From scattering theory, **spatial resolution** is expected to scale by a factor of 2

Gottschalk et al. (1993), Nucl. Instrum. Methods Phys. Res. B 74, 467-490; Scheidenberger et al (1996), Phys. Rev. Lett. 77, 3987-3990; Schardt et al (2010), Rev. Mod. Phys. 82, 383-425; Durante and Paganetti (2016), Rep. Prog. Phys. 79, 096702; Volz (2021), PhD thesis, Uni Heidelberg

Phase-II pCT scanner

- The **phase-II pCT scanner** was built in a collaboration of Loma Linda University (LLU) and the University of California at Santa Cruz (UCSC)
- Several successful experiments Northwestern Medicine Chicago proton center and Heidelberg Ion-Beam Therapy Center (HIT) mainly with protons but extension to helium ions
- In particular, the ΔE-E filter as introduced by Volz et al 2018 allows the successful application of the phase-II pCT scanner to helium ions; this filter was implemented in the reconstruction for this study
- Detailed Geant4 Monte Carlo model which is validated against experimental proton beam data and used for the characterisation and optimisation of the scanner

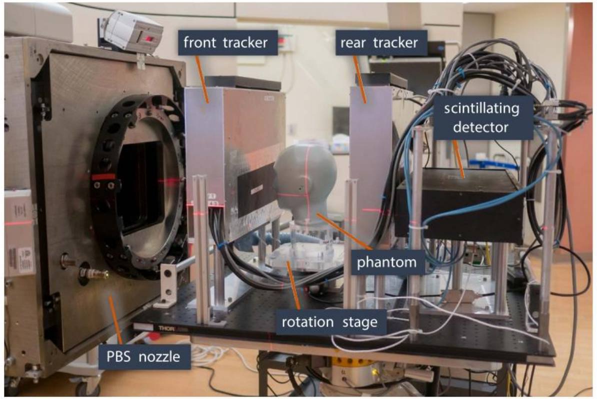

Dickmann et al (2020), Phys. Med. Biol. 65, 195001

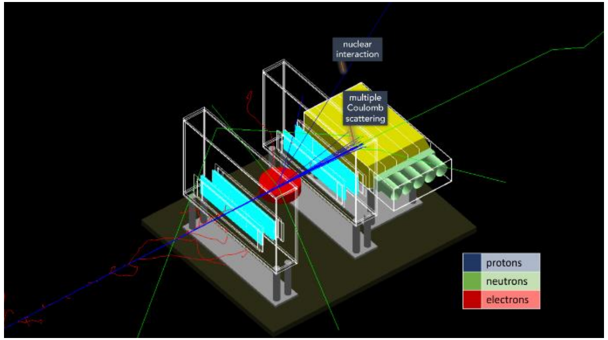

Dickmann (2021), PhD thesis, LMU

Johnson et al. (2016), IEEE 63, 52-60; Bashkirov et al. (2016), Med. Phys. 43, 664-674; Giacometti et al. (2017), Med. Phys. 44, 1002-1016; Dedes et al. (2017), Phys. Med. Biol. 62, 6026; Volz et al. (2018), Phys. Med. Biol. 63, 195016; Dedes et al. (2019) Phys. Med. Biol. 64, 165002; Dickmann et al. (2019), Phys. Med. Biol. 64, 145016; Dickmann et al. (2020), Med. Phys. 47, 1895-1906; Dickmann et al. (2020), Phys. Med. Biol. 65, 195001; Dickmann et al. (2021), Physica Medica 81, 237-244; Dickmann et al. (2021), Phys. Med. Biol. 66, 064001; Dickmann et al. (2021), Physica Medica 86, 57-65; Volz et al. (2021), Phys. Med. Biol. 66, 235010; Bär et al. (2022), Med. Phys. 49, 474-487; Dedes et al (2022), Zeitschrift für Medizinische Physik 32, 23-38;

Phase-II pCT scanner

Detailed Geant4 Monte Carlo model which allows simulating highly realistic data for the phase-II pCT scanner prototype build at Loma Linda University (LLU) and the University of California at Santa Cruz (UCSC)

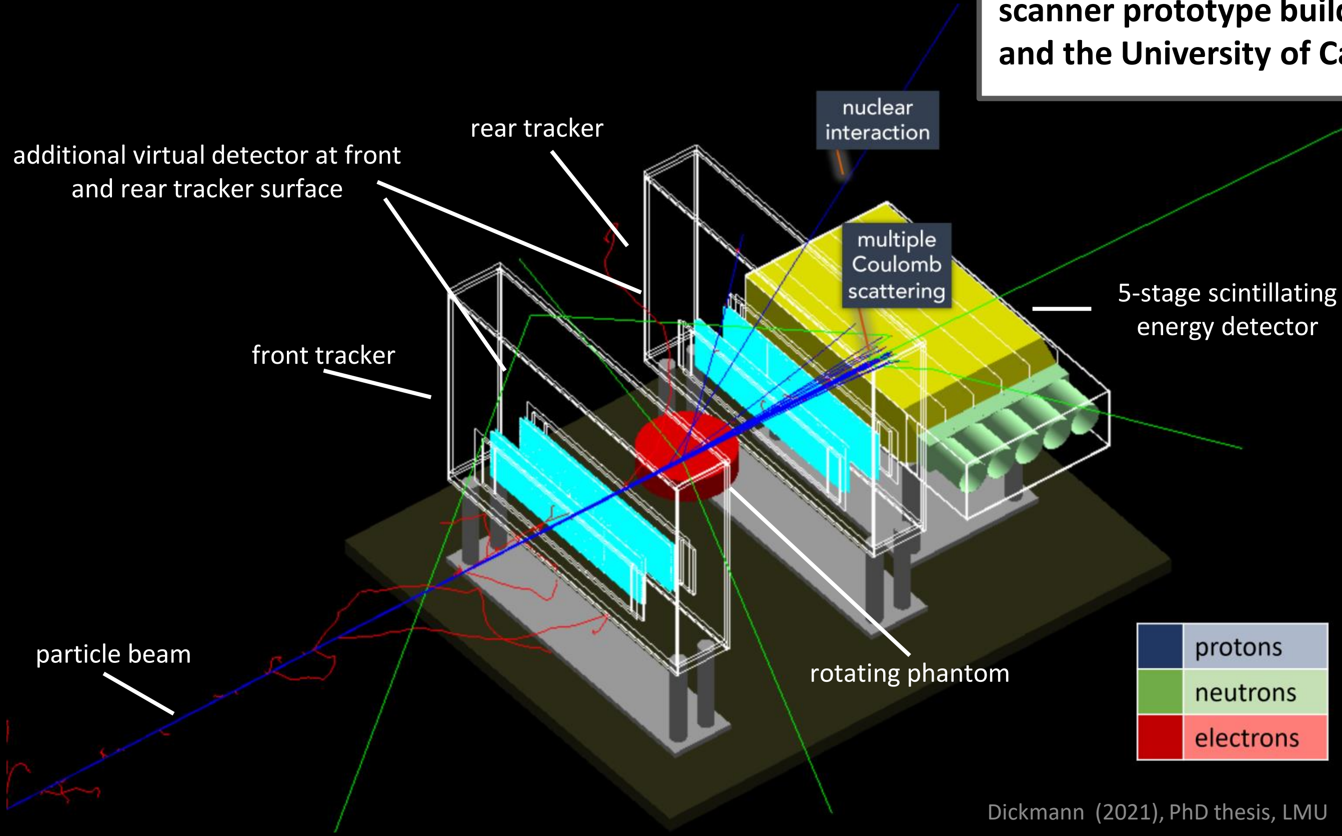

Dickmann (2021), PhD thesis, LMU

Volz et al. (2018), Phys. Med. Biol. 63, 195016

Dickmann et al (2019), Phys. Med. Biol. 64, 145016

Johnson et al. (2016), IEEE 63, 52-60

Bashkirov et al. (2016), Med. Phys. 43, 664-674

Giacometti et al. (2017), Med. Phys. 44, 1002-1016

Phantoms

Spatial resolution	Dose and image variance	Dose and image variance		RSP accuracy
(a) resolution phantom	**(b)** water phantom	**(c)** head phantom	**(d)** head phantom	**(e)** sensitometry phantom

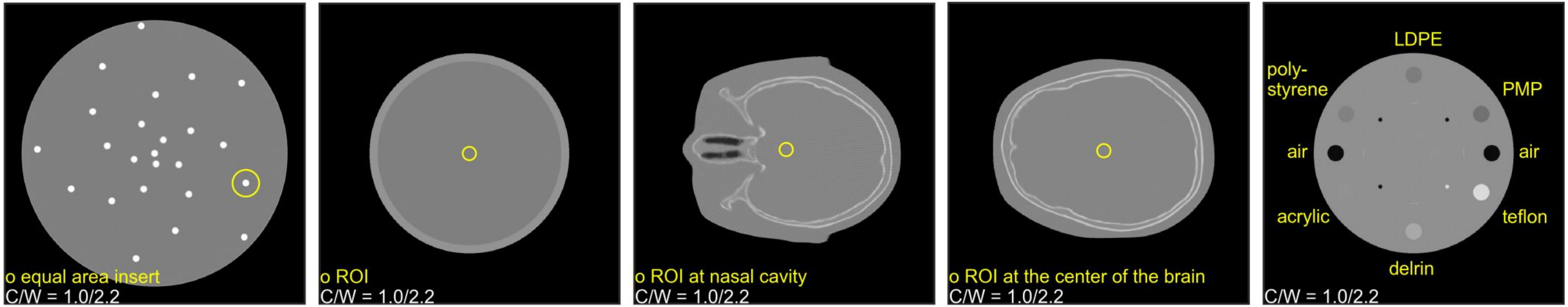

Götz et al. (2022), Phys. Med. Biol. 67, 055003

200mm diameter water cylinder with aluminium rods of 5mm diameter

Rit et al. (2013), Med. Phys. 40, 031103

Cylindrical PMMA shell of 150.5mm outer diameter that is filled with water

Pediatric head phantom mimicking a 5-year-old child using tissue equivalent materials (ATOM®, Model 715 HN, *CIRS Inc.*, Norfolk, VA)

ATOM®, Model 715 HN, *CIRS Inc.*, Norfolk, VA
Giacometti et al. (2017), Physica Medica 33, 182-188

150mm epoxy body containing 8 inserts of 12.2mm diameter with different materials

CTP404 module of the Catphan®600 phantom, *The Phantom Laboratory,* New York, USA

Spatial resolution

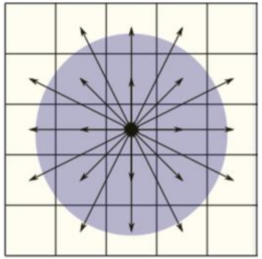

Fit to image intensity

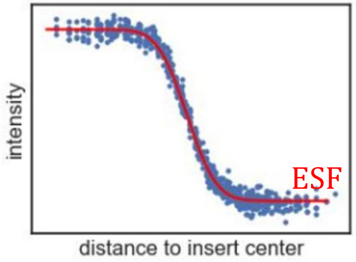

- **Spatial resolution** corresponds to the 10% level of the modulation transfer function (MTF)

$$f_{\mathrm{MTF10\%}} = \frac{1}{\pi\sigma}\sqrt{\frac{\ln 10}{2}}$$

where σ is obtained from the edge spread function (ESF)

$$\mathrm{ESF}(r) = \frac{A}{2}\left(1 + \mathrm{erf}\left(\frac{r-\mu}{\sqrt{2}\,\sigma}\right)\right) + C$$

Richard et al. (2012), Med. Phys. 39, 4115-4122 ; Krah et al. (2018), Phys. Med. Biol. 63, 135013; Khellaf et al . (2020), Phys. Med. Biol. 65, 105010

Native spatial resolution

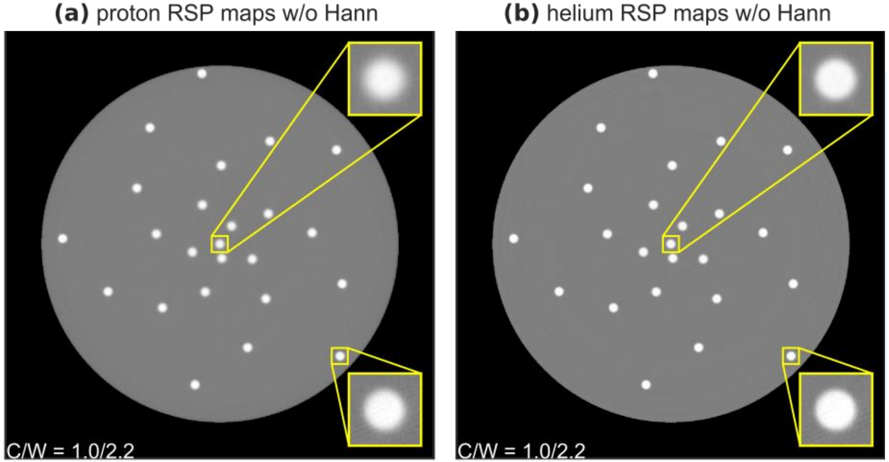

Götz et al. (2022), Phys. Med. Biol. 67, 055003

$$f^{\mathrm{centre}}_{\mathrm{MTF10\%}} = 0.48\,\frac{\mathrm{lp}}{\mathrm{mm}}$$
$$f^{r=92\mathrm{mm}}_{\mathrm{MTF10\%}} = 0.77\,\frac{\mathrm{lp}}{\mathrm{mm}}$$

$$f^{\mathrm{centre}}_{\mathrm{MTF10\%}} = 0.86\,\frac{\mathrm{lp}}{\mathrm{mm}}$$
$$f^{r=92\mathrm{mm}}_{\mathrm{MTF10\%}} = 1.09\,\frac{\mathrm{lp}}{\mathrm{mm}}$$

Dose and image variance

- **Variance maps** obtained from the variance reconstruction algorithm of Rädler et al (2018)

Rädler et al (2018), Phys. Med. Biol. 63, 215009

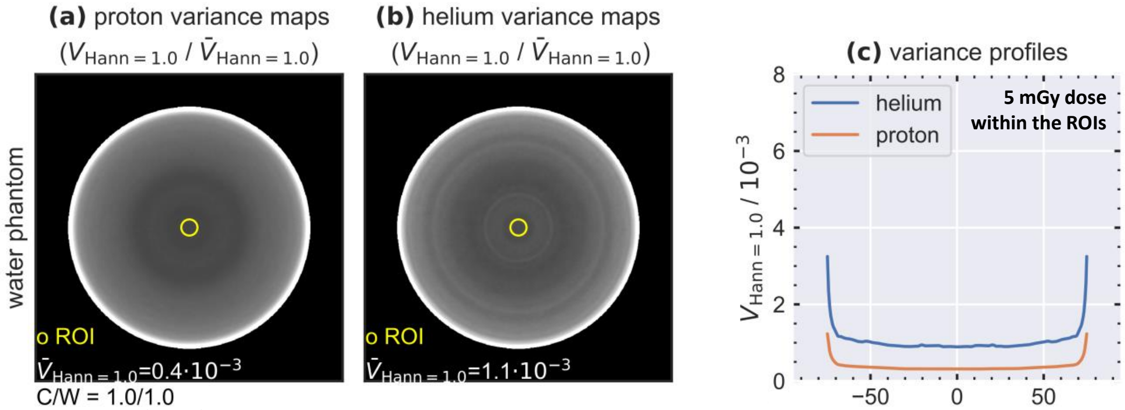

Götz et al. (2022), Phys. Med. Biol. 67, 055003

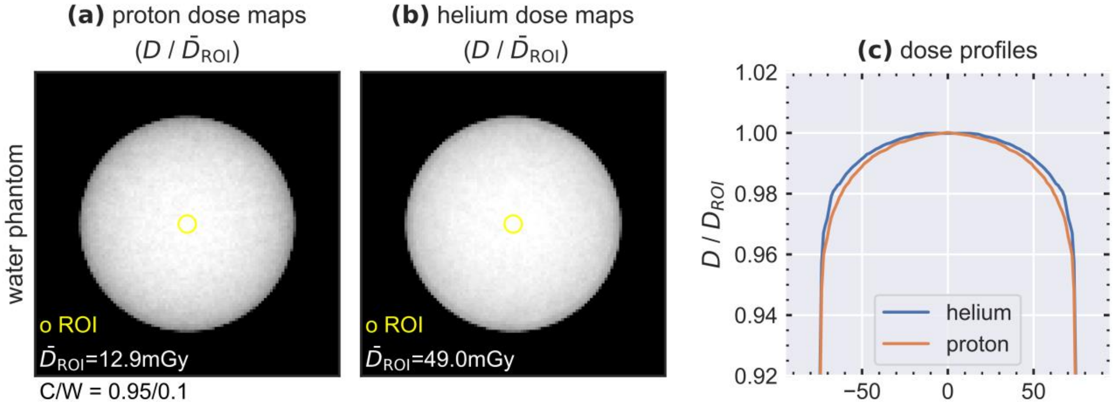

Götz et al. (2022), Phys. Med. Biol. 67, 055003

ROI	Dose ratio (He/p)	pCT dose (mGy)	HeCT dose (mGy)
Water phantom	2.9	5.00	14.29
Nasal cavity	2.9	11.29	32.34
Centre of brain	2.8	5.52	15.31

at equal image variance

Götz et al. (2022), Phys. Med. Biol. 67, 055003

Realistic and ideal data

- The additional virtual front and rear trackers in the simulation of the phase-II pCT scanner prototype allow the detection of the imaging particles without introduced uncertainties from the real trackers and the energy detector (ideal data)

ROI	Realistic dose ratio (He/p)	Ideal dose ratio (He/p)
Water phantom	2.9	1.3
Nasal cavity	2.9	2.1
Centre of brain	2.8	1.3

at equal image variance

Götz et al. (2022), Phys. Med. Biol. 67, 055003

Spatial resolution ratio (He/p)	Realistic	Ideal
Central insert of resolution phantom	1.8	2.0
Insert at $r = 92\text{mm}$	1.4	1.4

Götz et al. (2022), Phys. Med. Biol. 67, 055003

Native spatial resolution (ideal data)

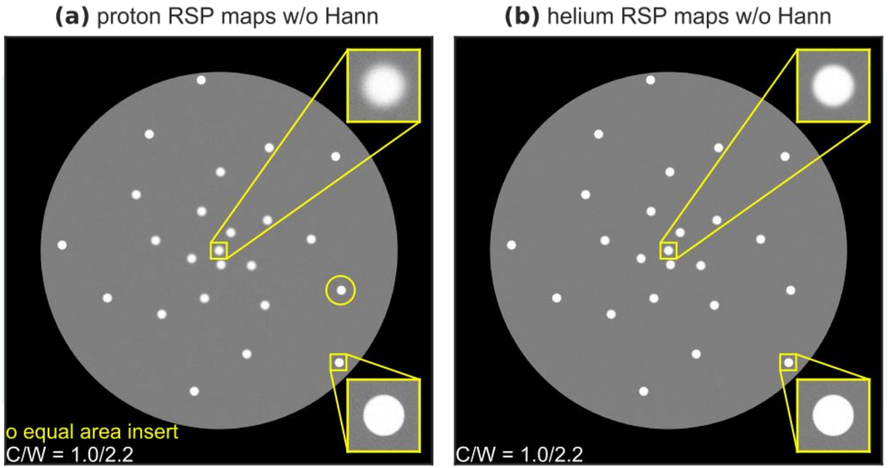

Götz et al. (2022), Phys. Med. Biol. 67, 055003

$$f_{\mathrm{MTF10\%}}^{\mathrm{centre}} = 0.59\,\frac{\mathrm{lp}}{\mathrm{mm}}$$

$$f_{\mathrm{MTF10\%}}^{\mathrm{r=92mm}} = 3.99\,\frac{\mathrm{lp}}{\mathrm{mm}}$$

$$f_{\mathrm{MTF10\%}}^{\mathrm{centre}} = 1.21\,\frac{\mathrm{lp}}{\mathrm{mm}}$$

$$f_{\mathrm{MTF10\%}}^{\mathrm{r=92mm}} = 5.42\,\frac{\mathrm{lp}}{\mathrm{mm}}$$

Hann windowing of reconstruction filter

- Modification of image noise and spatial resolution by replacing the **Ram-Lak filter** in the filtered backprojection reconstruction algorithm by the **Hann filter**

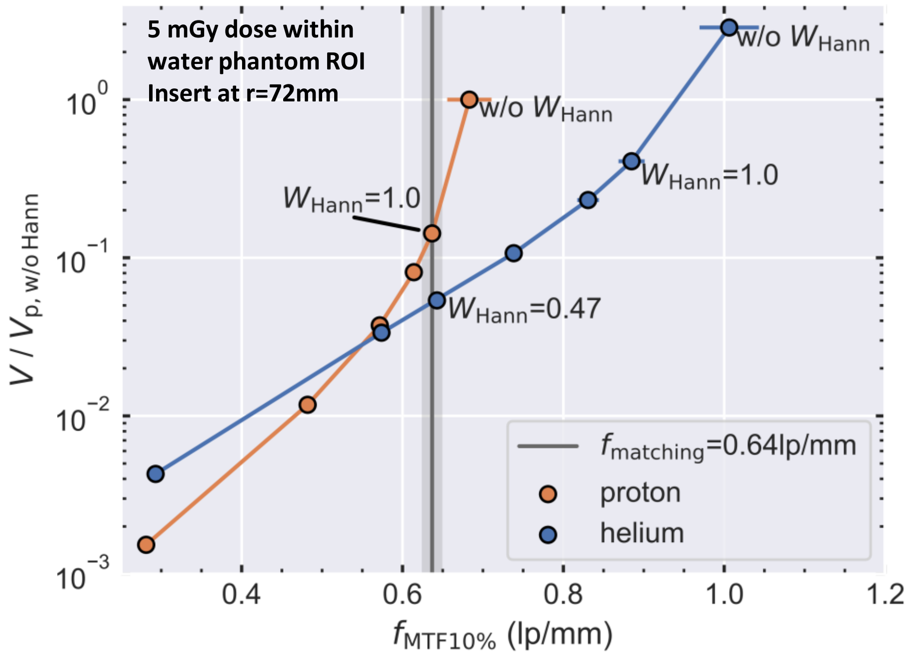

Götz et al. (2022), Phys. Med. Biol. 67, 055003

Ram-Lak filter

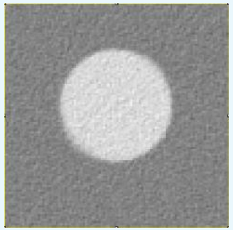

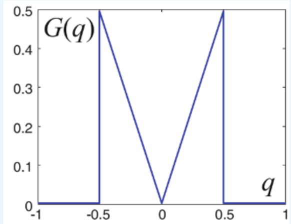

Buzug (2008), Computed tomography

$$G(q) = |q|\mathrm{rect}(q)$$

Hann filter

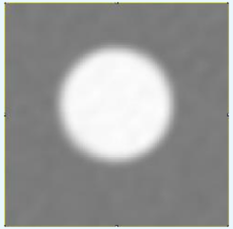

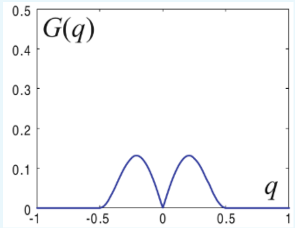

Buzug (2008), Computed tomography

$$G(q) = |q|\mathrm{rect}\left(\frac{q}{W_{\mathrm{Hann}}}\right)\left(0.5 + 0.5\cos\left(\frac{\pi q}{W_{\mathrm{Hann}}}\right)\right)$$

Spatial resolution and variance matching scenario

Spatial resolution

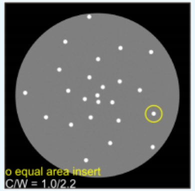

- Determination of Hann window W_{Hann} for equal **spatial resolution** at the equal area insert ($r = 72\text{mm}$) whose distance to the resolution phantom's centre divides the phantom in a circular area and a ring of approximately equal area

Image variance & dose

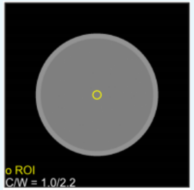

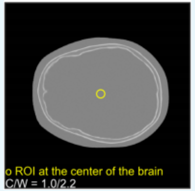

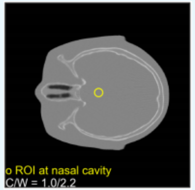

- Determination of dose and **image variance** in a ROI of 1cm diameter
- Rescaling of dose and image variance according to

$$V \cdot D = \text{constant}$$

  to a reference variance value
- The reference variance value corresponds to the variance within the central ROI of the water phantom at a proton dose of 5mGy and $W_{\text{Hann}} = 1.0$
- Comparison of the **dose** between pCT and HeCT scans

Spatial resolution matching

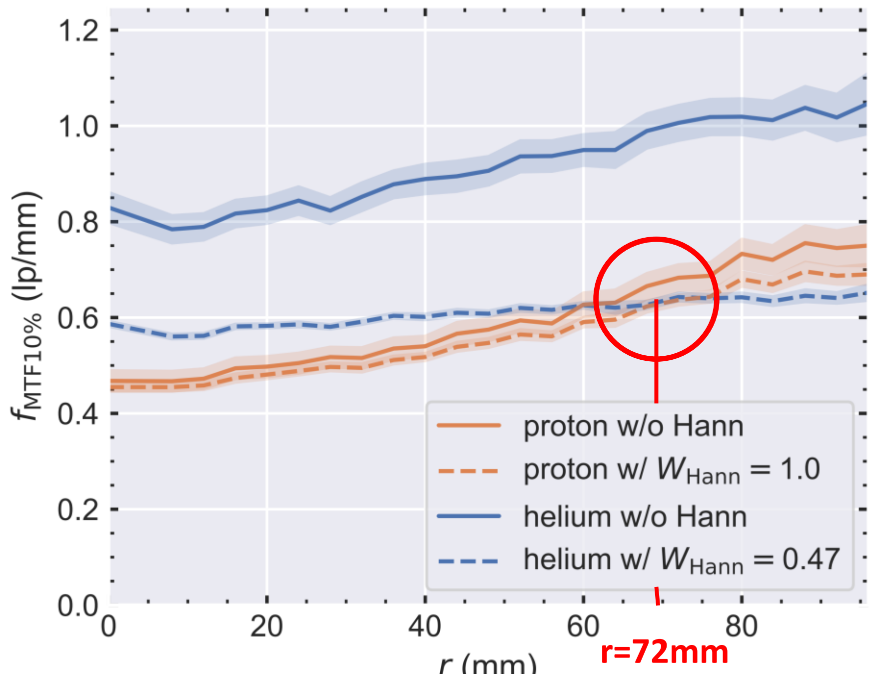

Götz et al. (2022), Phys. Med. Biol. 67, 055003

Spatial resolution matching with Hann filter

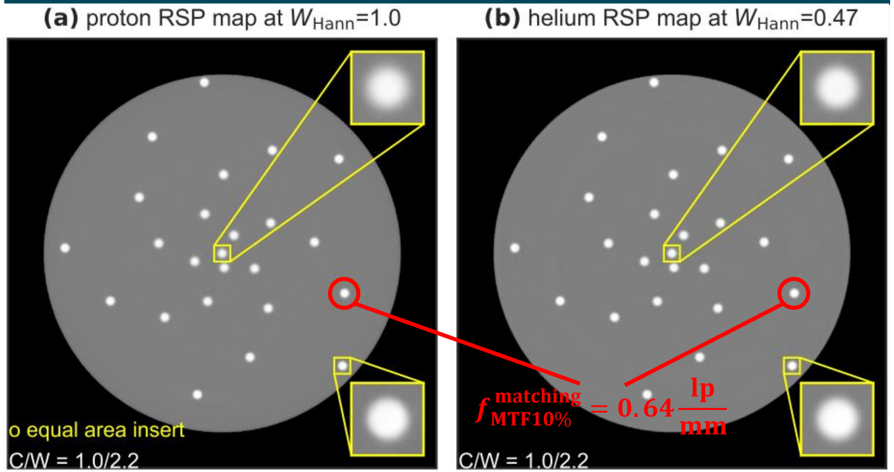

Götz et al. (2022), Phys. Med. Biol. 67, 055003

$$f^{centre}_{MTF10\%} = 0.45 \frac{lp}{mm}$$
$$f^{r=92mm}_{MTF10\%} = 0.69 \frac{lp}{mm}$$

$$f^{centre}_{MTF10\%} = 0.59 \frac{lp}{mm}$$
$$f^{r=92mm}_{MTF10\%} = 0.64 \frac{lp}{mm}$$

Spatial resolution and variance matching

- Application of the **Hann filter** for matched spatial resolution
- Variation of **dose** for equal image variance

ROI	dose ratio (He/p)	pCT dose (mGy)	HeCT dose (mGy)
Water phantom	0.38	5.00	1.89
Nasal cavity	0.38	11.28	4.24
Centre of brain	0.36	5.52	2.01

Götz et al. (2022), Phys. Med. Biol. 67, 055003

RSP accuracy

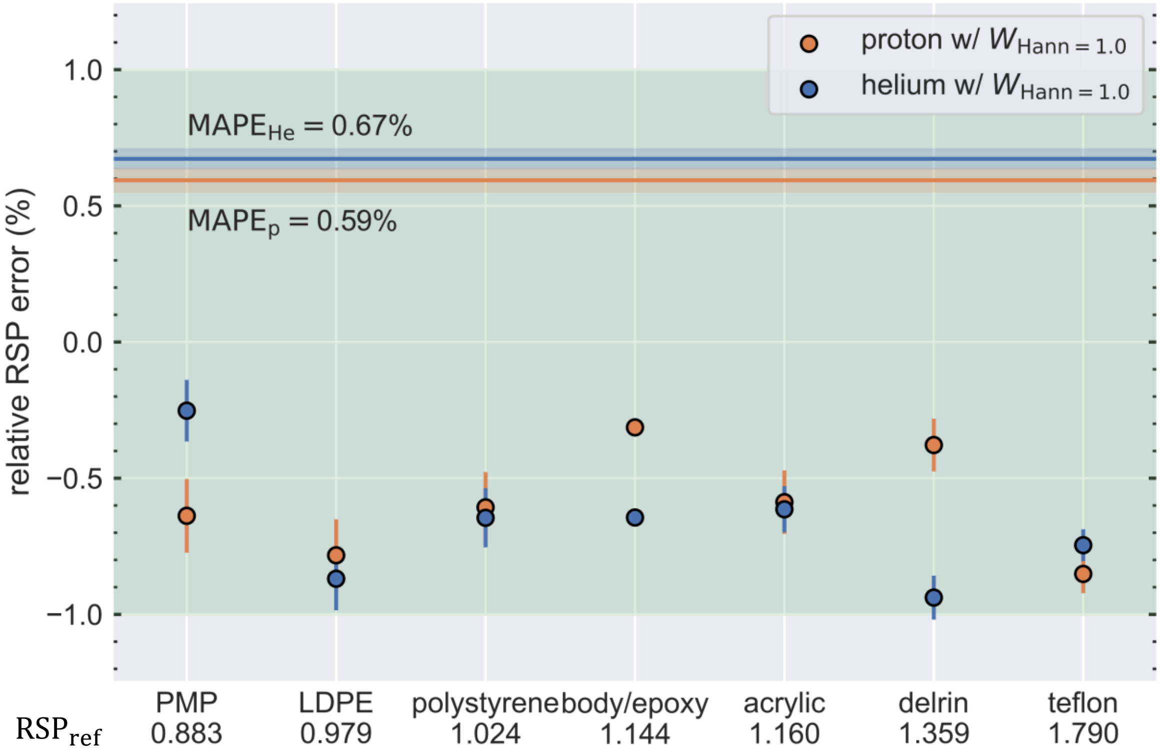

Götz et al. (2022), Phys. Med. Biol. 67, 055003

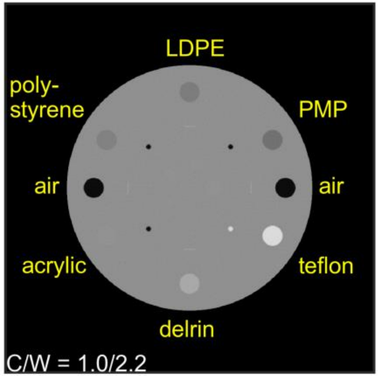

Götz et al. (2022), Phys. Med. Biol. 67, 5

Relative RSP error δ_{RSP}

$$\delta_{RSP} = 100\% \cdot \frac{RSP_{mean} - RSP_{ref}}{RSP_{ref}}$$

Mean absolute percent error MAPE

$$MAPE = \frac{1}{M} \sum_{m=1}^{M} |\delta_{RSP,m}|$$

Conclusions

- Helium has a higher **spatial resolution** by a factor of 1.8 (phantom centre) compared to protons
- Helium requires 2.8-2.9 times the proton dose for equal **image variance**
- At **spatial resolution and variance matching,** helium requires only 0.38 times the proton dose
- **Relative RSP error** as obtained from the sensitometry phantom is below 1% with $\mathrm{MAPE_p}$=0.59% and $\mathrm{MAPE_{He}}$= 0.67%
- **Theoretical predictions** which expect a spatial resolution advantage by a factor of 2 for helium ions and a higher image variance by only 20% in HeCT compared to pCT at the same dose indicate potential for improvement in HeCT

HeCT is expected to reduce dose exposure of patients with image noise equal to pCT, good spatial resolution and acceptable RSP accuracy

- However, experimental validation is still required
- Further optimisation of the scanner to helium as well as extending this study to image artefact correction methods may modify and improve the results

Thank you for your attention!

LMU LUDWIG-MAXIMILIANS-UNIVERSITÄT MÜNCHEN

LMU KLINIKUM

CREATIS

UNIVERSITÉ DE LYON

LOMA LINDA UNIVERSITY

Deutsche Forschungsgemeinschaft